High Energy Density Matter Generated by Heavy-Ion Beams, and Application to Fusion Energy

A. Blazevic[1], B. Rethfeld[1] and D.H.H. Hoffmann[1,2,⋆]

[1]Gesellschaft für Schwerionenforschung mbH
GSI-Darmstadt, Plasmaphysik
Planckstr. 1, 64291 Darmstadt, Germany
[2]Institut für Kernphysik, Technische Universität Darmstadt
Schlossgartenstr. 9, 64289 Darmstadt, Germany

Abstract

A detailed understanding of interaction phenomena of intense ion- and laser radiation with matter is important for a large number of applications in different fields of science, from basic research of plasma properties to application in energy science. Energy loss processes of heavy ions in plasma and cold matter are important for the generation of high energy density states in general and especially in the hot dense plasma of an inertial fusion target. Of special interest are phase transitions and the associated time scales when matter passes the warm dense matter regime of the phase diagram at high density but relatively low temperature. We present an overview on recent results and developments of beam plasma, and beam matter interaction processes studied with heavy ion beams from the GSI accelerator facilities.

Contents

⋆ E-mail: d.hoffmann@gsi.de

1. Introduction

The early theoretical work by Bethe (1930, 1932), Bloch (1933) and later Bohr (1948) paved the ground for a theoretical understanding of ion-matter interaction and the stopping power of matter. Since the discovery of fission fragments in the beginning of the 20th century the interaction of heavy ions with solid or gaseous matter has been investigated intensively in experiments, resulting in a vast number of semi- or empirical formulas, tables or codes for the mean charge of the projectile, its charge state distribution or the stopping power (Lindhard and Scharff, 1961; Northcliffe and Schilling, 1970; Ziegler et al., 1985; Hubert et al., 1990; ICRU, 2005). Despite the vast amount of theoretical and experimental work, a proper general microscopic description of the physical processes is still lacking or at least needs improvement.

Even less is known about the details of the interaction of ions with plasmas, a field with increasing interest especially for astrophysics, where plasma is the usual state of matter. Fusion physics is another field that shows great interest for beam plasma interaction since accelerators are a candidate for a primary driver in inertial confinement fusion, ICF-scenario, where a small pellet, filled with a deuterium-tritium mixture, is heated by X-rays in a hohlraum. The X-rays can be generated by powerful lasers, Z-pinches or by ion-beam interaction with matter. In the latter case the ion beam is stopped in a converter target and its energy is converted into X-rays. During the stopping process of an intense bunch of ions the converter target will be heated to approximately 300 eV in about 10 ns. Therefore the major part of the ion beam energy is deposited into hot and dense matter,

which is then a partially ionized plasma. For the optimization of the converter parameters a detailed knowledge of the ion-plasma interaction is needed (Badger et al., 1990).

2. Accelerator and Laser Facilities at GSI-Darmstadt

The perspectives of intense ion beams to drive an inertial fusion targets motivated a number of major accelerator laboratories like LBNL-Berkeley, ITEP-Moscow, TIT-Tokyo, University of Paris, Orsay and GSI-Darmstadt to start plasma physics research programs to study the interaction of heavy ion beams with ionized matter (Logan et al., 2006; Roy et al., 2005; Sharkov et al., 2005; Someya, 2006; Oguri et al., 2005; Gardes et al., 1989; Deutsch et al., 1989; Hoffmann et al., 2005). Today, the GSI-heavy ion accelerator laboratory in Germany operates the most powerful and versatile heavy ion accelerator worldwide and in addition to this there is an approved project to build a new accelerator facility at GSI called FAIR (Facility for Antiproton and Ion research). This new accelerator (Figure 1) will consist of two powerful heavy ion synchrotrons and a number of storage rings and experimental facilities for various research projects. The centerpiece of the accelerator assembly will be a 100 Tm heavy ion synchrotron. This will extend the available beam deposition power from the current level of 50 GW/g by at least two orders of magnitude up to 12000 GW/g. Many aspects of high power beam physics associated with inertial confinement fusion driven by intense heavy ion beams can be addressed there, even though this facility will not provide enough beam power to ignite a fusion pellet.

GSI-Darmstadt is also the first accelerator laboratory where in addition to a powerful and intense heavy ion beam a high-energy laser beam is available for experiments using laser and particle beams simultaneously. The already existing laser facility nhelix (nanosecond high energy laser for ion experiments) is currently complemented by a new laser PHELIX (Petawatt High Energy Laser for Ion Experiments). This is a laser system in the kJoule regime with the option to produce ultra-short, high-intensity light pulses with a total power above 1 PW (10^{15} Watt). It will be able to produce a light pulse pressure exceeding the pressure in the interior of the sun. The full potential of the PHELIX laser will be exploited in high energy density physics experiments with the high intensity heavy ion beams of the future accelerator at GSI. The unique combination of ion and laser beams facilitates novel and pioneering beam-plasma interaction experiments to investigate the structure and the properties of matter under extreme conditions of high energy density.

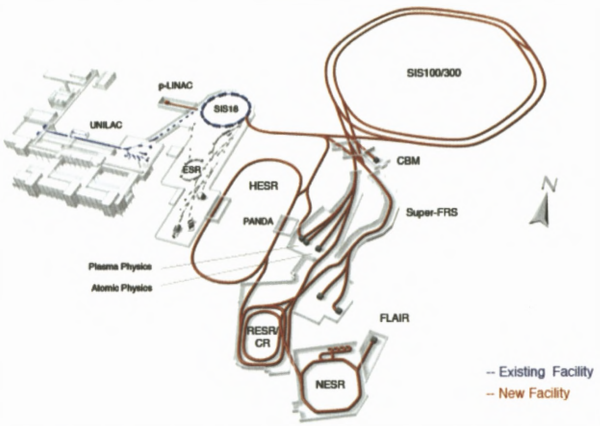

Figure 1. GSI accelerators and the experimental areas of plasma physics. The FAIR project at GSI will greatly improve the experimental option for beam-plasma experiments. The arrows point to the future experimental areas of plasma physics and atomic physics at FAIR.

3. Heavy Ion Plasma Interaction

Early stopping power experiments for protons and heavy ions in ionized matter have used discharge plasma and Z-pinch plasma as well as laser produced plasma (Ogawa et al., 2001; Belyaev et al., 1996; Couillaud, 1994; Gardes et al., 1988; Hoffmann et al., 1988). The most effective method to determine the ion energy loss was based on time-of-flight measurements where the rf-frequency of the accelerator was used for timing purposes. The experiments using gas discharge plasmas as stopping medium, reached densities up to 10^{17} free electrons/cm^3 and plasma temperatures of a few eV for hydrogen plasma (Hoffmann et al., 1990; Weyrich et al., 1989; Jacoby et al., 1995). The results show a clearly enhanced stopping power of the projectiles in the plasma compared to cold matter. In contrast to cold matter the projectiles do not interact with neutral atoms but with target ions and additionally with a free electron gas. Stopping power models applicable for this experimental situation can be based on theories given by Bethe, Bohr and Bloch, taking into account the Barkas corrections for the gas case. Since the Barkas correction nearly cancels out the Bloch ones we find that the situation for partially ionized plasmas can be well described in the frame of the standard stopping model, based on the Bethe formalism as suggested by Peter (1988):

$$-\frac{\mathrm{d}E}{\mathrm{d}x} = \frac{16\pi a_0^2 I_\mathrm{H}^2 Z_\mathrm{eff}^2}{m_\mathrm{e} v^2}\left[\sum_{Z=0}^{Z_\mathrm{t}}(Z_\mathrm{t}-Z)n_z \ln\left(\frac{2m_e v^2}{\bar{I}_Z}\right) + n_\mathrm{e}\ln\left(\frac{2m_\mathrm{e}v^2}{\hbar\omega_\mathrm{P}}\right)\right], \quad (1)$$

with a_0: the Bohr radius, I_H: the mean ionization potential of hydrogen, Z_{eff}^2: effective projectile charge, $m_e v^2$: electron mass times projectile velocity, Z_t: target atomic number, n_Z, n_e: density of plasma ions of charge Z and free electrons, respectively, $\bar{I}_Z$: the mean plasmon energy energy transfer in a collision with a plasma ion of charge Z, and $\hbar\omega_P$: the plasma frequency. The Coulomb logarithm is split up into two contributions. The first term describes the energy transfer to the remaining bound electrons in the plasma. As in a plasma a charge state distribution is created it is necessary to sum over all charge states Z and take into account the varying mean ionization potential of the different charge states. In the second term the contribution of free electrons is described. In this case the projectile can transfer its energy in collisions to free electrons and by plasmon excitation.

In the case of fully ionized plasma the first term of the equation given above is zero. This case prevails in our experiments with fully ionized hydrogen plasma from discharges and z-pinches, and we find that in this case the experimental data are well represented by the model given by Peter (1988). Figure 2 shows experimental data of energy loss measurements for Kr ions in cold hydrogen gas and fully ionized hydrogen plasma from discharge plasma. The red hatched area is the energy loss expected for Kr ions with different effective charge states. The blue graph represents Northcliffe and Schilling stopping values.

Mainly two effects contribute to the stopping power enhancement of ions in fully ionized hydrogen plasma:

(a) An efficient energy transfer to the free electron gas.
For free electron densities below $10^{21}/cm^3$ the plasmon energy $\hbar\omega_P$ is less than 1 eV, thus much smaller than the average of the excitation or ionization energy of bound electrons in hydrogen. This leads to an increase of the stopping power by a factor of up to 2.5.

(b) An increase of the projectile charge state.
Since for a free electron it is nearly impossible to fulfill energy conservation and momentum conservation at the same time in a capture process, the dynamic equilibrium of capture and ionization processes is shifted towards a higher mean projectile charge state, which in turn leads to an increase of the effective charge Z_{eff}.

The stopping power of ionized matter depends strongly on Z_{eff}. There is no simple relation between Zeff and the charge state of the projectile. The experimental results and the arguments given above suggest however, that the charge state of an ion traversing fully ionized hydrogen plasma is higher than the charge state of the projectile under the same conditions of density in cold hydrogen gas.

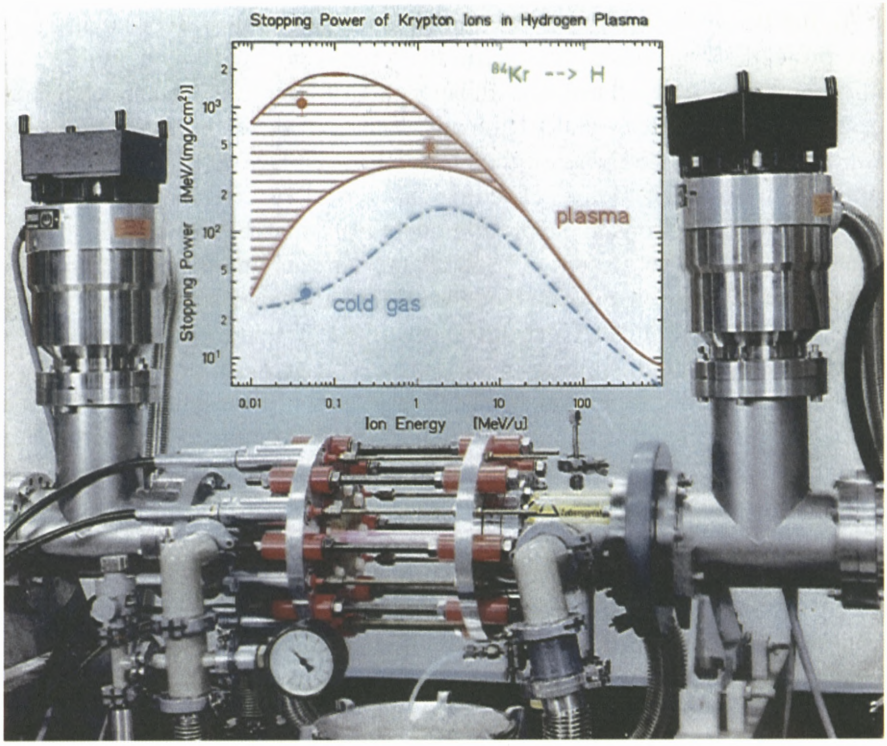

Figure 2. Hydrogen discharge plasma to provide fully ionized hydrogen plasma for plasma stopping power measurements. Red data points are stopping power data of plasma for Kr ions at 1.4 MeV/u and 45 keV/u respectively. The blue data points represent data in cold hydrogen gas. (From Jacoby et al., 1995.)

In different laboratories experiments were carried out to measure and calculate the charge state of ions passing through ionized matter (Nardi et al., 2006; Kojima et al., 2002; Golubev et al., 2001; Dietrich et al., 1992). The GSI plasma physics group has dedicated their efforts to extend the experimental data base for the stopping power of ions in plasmas to higher densities and higher temperatures. At the experimental area Z6, a branch of the UNILAC (Universal linear accelerator), an experimental setup has been built up for the investigation of the interaction of ions with laser produced plasmas. Therefore a thin foil, mainly a carbon foil with a thickness of a few hundred μg/cm^2, is irradiated by the nhelix laser (amplified NdYAG laser with $\lambda = 1064$ nm, energy up to 100 J in 5–15 ns (FWHM)) transforming the foil into a dense and hot plasma with densities close to solid density and temperatures of over 200 eV in the very hot spot. As the plasma is expanding there will be density and temperature gradients, which have to be mea-

sured experimentally. At the same time an ion pulse with a length of a few hundred μs, built up of micro bunches with a length of 3 ns FWHM and a frequency of 108 MHz, is probing the plasma parallel to the laser direction. This means the expanding plasma is being investigated each 9.2 ns. The delay between the laser and the ion bunch can be shifted with an accuracy of 1 ns. The ions first penetrate a still cold part of the foil, and then enter dense and hot plasma, which is expanding and cooling. Finally all matter along the interaction path has vanished and the ions fly through vacuum with their initial energy. The energy loss as a function of time is determined by a time of flight measurement. Additionally a dipole magnet behind the target chamber can be used to measure the charge state distribution of each single bunch penetrating the plasma. As a result we obtain a set of energy loss data and charge state distributions of ions probing expanding plasma. As the target conditions with respect to density and temperature during the interaction time are important, a set of plasma diagnostic tools is used e.g. laser interferometry for a space resolved measurement of the free electron density n_e, time resolved X-ray spectroscopy for the temperature determination, a visible streak camera measuring the expansion velocity, pinhole cameras, etc. Nevertheless, the very dense and hot part of the plasma is not accessible with all these diagnostics. Therefore results of the plasma diagnostic serve to benchmark hydrodynamic simulation of the laser-matter interaction and plasma expansion. From these simulations the necessary density and temperature profiles along the ion path can be extracted for the theoretical calculation of the energy loss and charge state distributions.

4. Charge State Distribution of Heavy Ions Penetrating Thin Target Foils

The theoretical description of the charge state distributions faces the problem that until now no reliable theory or code to calculate all the relevant charge exchange cross sections exists. Therefore we used the high resolution spectrometer of the Hahn–Meitner Institut in Berlin to measure them along with energy loss data as a function of the projectiles charge state, to extract charge state dependent stopping powers $S(q)$. Measurements of this type have been pioneered at Harwell and Chalk River many years ago and were greatly improved by Ogawa et al. (1992, 1997) and references therein. Calculations have been carried out by Winterbon (1977), Sigmund (1992) and Sigmund and Schinner (2001) and references therein.

4.1. Experimental Setup

The investigated system was Argon interacting with thin Carbon target foils. The projectile energy was chosen to be 4 MeV/u, a suitable energy for the ion-plasma

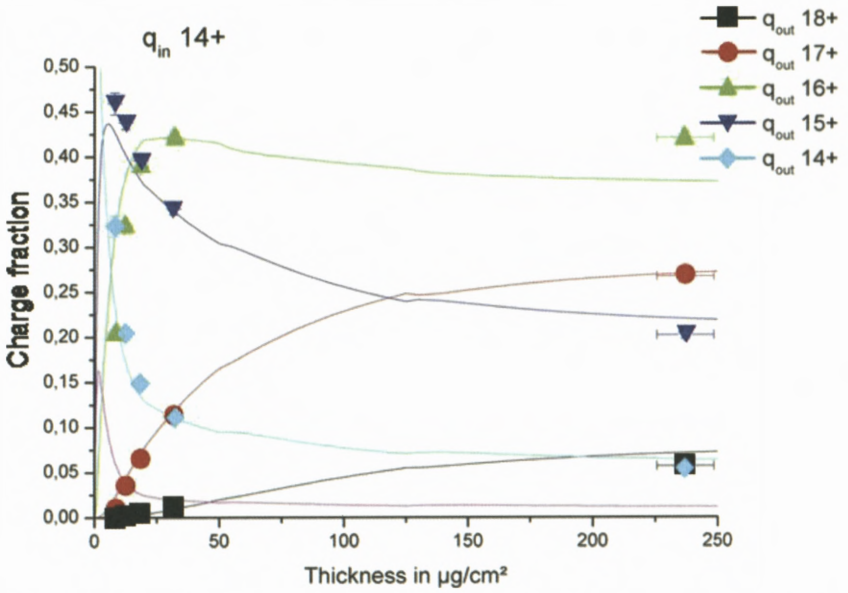

Figure 3. Evolution of the charge state distribution for Ar ions with the incoming charge $q_{\text{in}} = 14+$.

interaction experiments. The initial charge state was varied between 14+ and 18+, covering over 99% of the equilibrium charge state distribution of Ar at 4 MeV/u.

The thicknesses of the target foils were 8.1, 12, 18, 32.2 and 231.6 μg/cm^2, measured by the energy loss of α particles with energies of 5.80 and 5.76 MeV emerging from an open ^{244}Cm source. Such thin foils were used on the one hand to cover the pre-equilibrium region, so that the evolution of the charge state distributions can be measured to fix the charge exchange cross sections, on the other hand to measure a difference in the energy losses as function of the charge states, $\Delta E(q)$. We measured the evolution of the incoming charge states 14+, 16+ and 18+ using increasing foil thicknesses until charge state equilibrium is reached.

4.2. Charge State Distributions

In contrast to equilibrium charge state measurements, the pre-equilibrium region allows to determine the cross sections absolutely. Figures 3 to 5 show the evolution of the charge state distributions in this region for the three incoming charge states (symbols). To the statistical error, marked by the error bars, a systematic error of 3% must be added.

The interpretation of these results can be done by model calculations in two ways (Blazevic et al., 2000): (a) by solving the coupled-channel rate equations

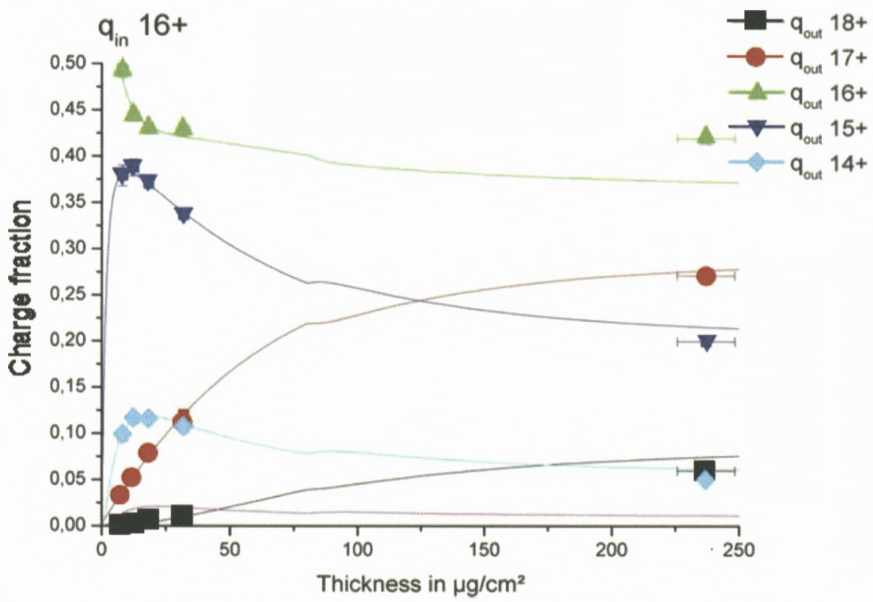

Figure 4. Evolution of the charge state distribution for Ar ions with the incoming charge $q_{\mathrm{in}} = 16+$.

for the individual charge state probabilities, or (b) by a Monte Carlo simulation following the history of each ion on its way through the foil. Both methods need a complete set of cross sections for all possible interactions between the projectile and the target atoms. In our studies both methods were applied. First the rate equation model will be described, which results are shown as lines in Figures 3 to 5.

The solving of the rate equations was performed with the ETACHA code of Rozet et al. (1996), taking into account the following processes for the first three projectile and target shells including the sub-shells:

- radiative and mechanical electron capture;
- ionization;
- excitation;
- radiative and Auger decay, auto ionization.

The cross sections enter into the rate equations, which can be written as

$$\frac{\mathrm{d}Y_i(x)}{\rho \cdot \mathrm{d}x} = \sum_j Y_j(x)\sigma_{ji} - Y_i(x)\sum_j \sigma_{ij}, \tag{2}$$

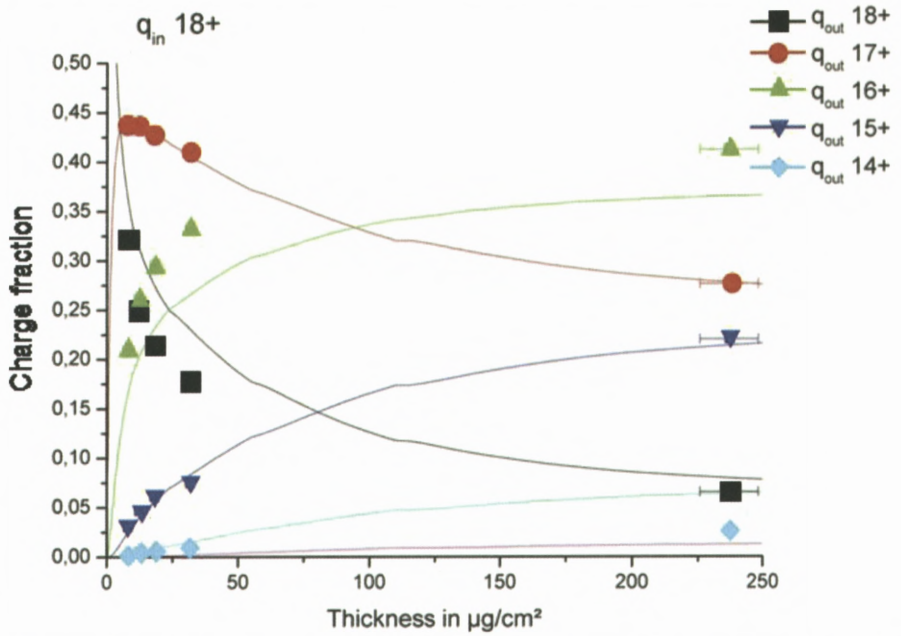

Figure 5. Evolution of the charge state distribution for Ar ions with the incoming charge $q_{\text{in}} = 18+$.

where $Y_i(x)$ denotes the fraction of ions in charge state i including excited states; x is the traversed target thickness and σ_{ij} denotes the collision cross section from state i to state j. The code calculates the cross sections for bare projectile ions in the case of capture processes or a hydrogen like configuration for the ionization, excitation and decay processes, taking into account the screening effects of the residual electrons. As the code was initially written for energies above 10 MeV/u, it had to be adapted to the experimental situation. In contrast to the equilibrium charge distributions, the data for the pre-equilibrium region allows to determine absolute values for the cross sections. Figures 3–5 show that charge state equilibrium of Ar ions is obtained with carbon foils of more than 200 μg/cm^2.

The analysis results in a set of cross sections, which were used in our Monte Carlo Simulation to describe the charge exchange processes inside the foil. From these calculations we deduce, that even for the thinnest foil and an initial charge state of $q_{\text{in}} = 16+$ far less than half of all ions keep their charge state during the passage through the foil. Therefore no measured charge state dependent parameter can be regarded as "frozen charge state" result.

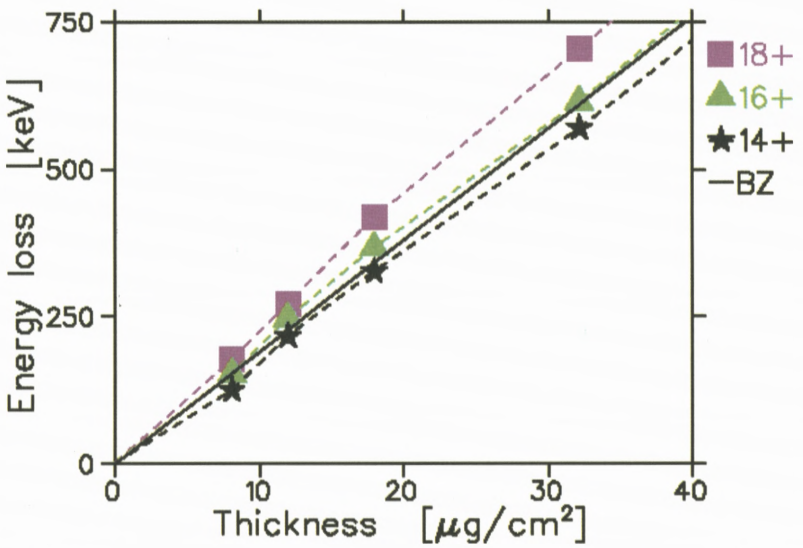

Figure 6. Measured energy loss for varying incoming charge states, $\Delta E(q_{\text{in}} = q_{\text{out}})$, of Argon projectiles at 4 MeV/u penetrating Carbon foils. BZ corresponds to energy loss calculations with the Biersack–Ziegler code SRIM.

4.3. Charge State Dependent Energy Loss

The magnetic field of the spectrometer selects a specific charge state for energy loss measurements. Figure 6 shows the $\Delta E(q_{\text{in}} = q_{\text{out}})$ results for thin foils and charge states from 14+ to 18+. As discussed above, these values are not generated by the "frozen charge state", since the majority of ions have undergone several charge state fluctuations before leaving the foil with q_{out}. As described in detail in Blazevic et al. (2002), we have developed an iterative Monte Carlo simulation method to eliminate the influence of the charge exchange and to extract "frozen charge state" stopping powers $S(q)$. In other words, we used the charge exchange cross sections from the charge state distribution measurements, combined them with charge dependent stopping powers and succeeded to reproduce the measured energy losses including all the charge exchange effects. The result is plotted in Figure 7.

These data can now be used to test some theoretical calculations of the $S(q)$ values. Four of them shall be discussed below:

- Kaneko derived an analytical formula for $S(q)$ for swift lithium- and beryllium-like ions based on first-order perturbation theory. The bound

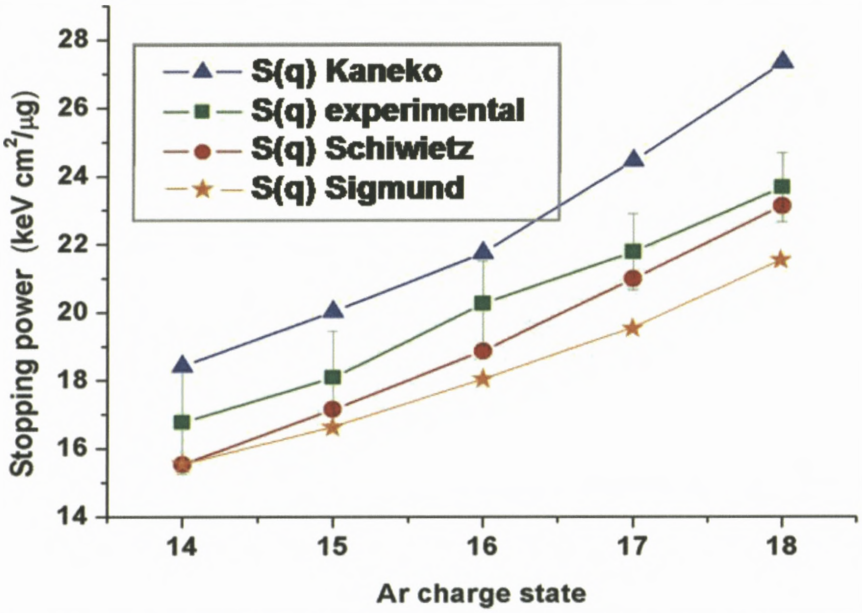

Figure 7. Experimental and theoretic charge state dependent stopping power $S(q)$ for Argon ions interacting with Carbon.

electrons attached to the ion in the ground state were described by the Hartree–Fock–Slater determinant (Kaneko, 1994).

- Schiwietz and Grande developed the CASP code to calculate the impact parameter dependence of the electronic energy loss of bare ions. This perturbative convolution approximation is based on first order perturbation theory, which is only valid for fast projectiles with low charges. But using Bloch's stopping power results and a scaling, they could overcome these restrictions and derived a unitary convolution approximation (Schiwietz and Grande, 1999).
- Maynard expressed the stopping power of swift heavy ions within the convergent kinetic Lindhard theory, based on a modified Bloch correction term, devoted to correctly describe the close collisions contribution to the energy loss process (Maynard et al., 2001).
- Sigmund and Schinner treated charged particle stopping via a binary scattering theory, assuming free binary collisions governed by a suitable effective potential (Sigmund and Schinner, 2000).

Kaneko's first order perturbation theory is known to overestimate the $S(q)$ values for heavier projectiles, so it can be seen as an upper limit. On the other hand

the theory of Schiwietz and Grande lacks some correction terms, which should increase the calculated stopping powers; hence it is a lower limit for the $S(q)$ values. Our experimental data are between these limits.

5. Timescales of Phase Transitions from Solid to Warm Dense Matter

In order to be able to study the stopping power of ions in laser-generated plasmas, knowledge of the transient material state of the laser-irradiated target foil, which is initially in solid state, is essential. Numerical codes, simulating the interaction of the target with the laser and the subsequent hydrodynamic expansion, usually assume a cold plasma as initial condition. However, the transition from solid to warm dense matter may proceed through different pathways and may be completed on different timescales, depending on target material and energy of excitation. Here, we can benefit from experimental and theoretical studies on the dynamics of a solid during and after irradiation with an ultrashort laser pulse. Examples of such studies will be reviewed below.

The time-resolved description of the excitation of the solid and the induced phase transitions is a challenging task: On ultrashort time scales the highly excited material passes through non-equilibrium states of different kinds. Therefore, the theoretical description of the investigated processes may differ strongly from the classical descriptions valid for equilibrium or steady-state conditions. A temporal separation of the basic processes as excitation, melting and material removal can be achieved, applying an ultrashort laser pulse of about a hundred femtosecond duration. This allows a separate investigation of each of these key-processes.

Figure 8 shows a schematic view of the typical time scales and intensity ranges of some phenomena, discussed in the following. The pathway of the material after irradiation depends strongly on the type of material and on laser properties as intensity and wavelength. Note that in real laser experiments due to laser intensity variations in space, as well as for excitation with ion beams, a large variety of these phenomena (and probably further transient states and pathways which are not shown) may play a role leading to a rather complex behaviour.

5.1. Absorption of Energy within the Solid

Heavy ions of sufficient high energy lose energy within solid material through electronic stopping, thus the energy input proceeds by heating of the electron gas of the solid. Also laser energy absorption is usually dominated by free carrier absorption. In metals, free electrons are inherent in the conduction band of the metal. At moderate intensities, these electrons absorb photons and thus gain higher energy. Following absorption, this energy is transferred from electrons to phonons by

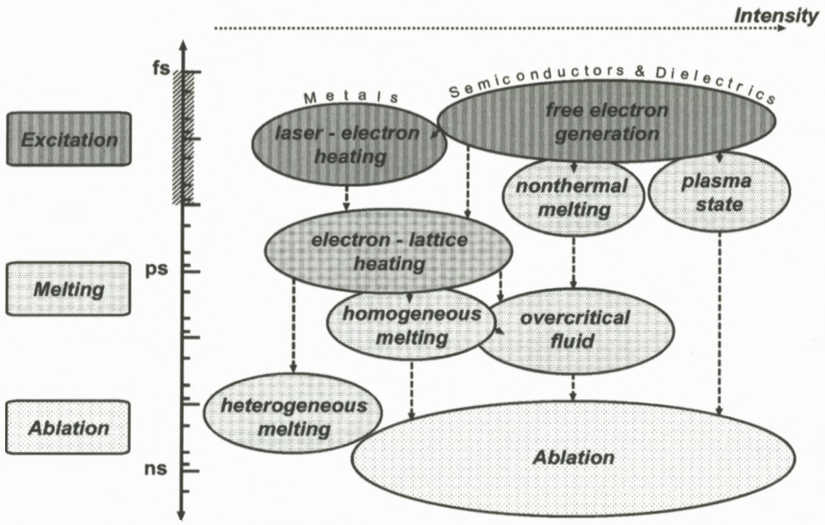

Figure 8. Schematic view of typical time scales and intensity ranges of some phenomena occurring during and after irradiation of a solid with an ultrashort laser pulse of about 100 fs duration. Excitation occurs during irradiation, while the time scale of melting may vary for different processes depending on excitation strength. Material removal, i.e. ablation, lasts up to the nanosecond regime (Rethfeld et al., 2004). The intensities, this overview applies to, ranges from about 10^{10} to 10^{14} W/cm^2.

electron-phonon interaction, that is, lattice heating occurs. For timescales longer than the electron-electron collision time, the two-temperature model (Kaganov et al., 1957; Anisimov et al., 1974) provides an applicable description for the heat transfer and heat conduction for the case of laser irradiation as well as for the case of ion impact.

If the timescale of interest is shorter or in the range of the electron-electron thermalization time, the two-temperature model is not applicable at first. We have extensively studied the dynamics of laser-excited electrons in this regime, including the influence of a nonequilibrium electron distribution on the electron-phonon energy transfer (Rethfeld et al., 2002b).

In dielectrics there is only a negligible amount of free electrons inherent in the conduction band. However, in the case of irradiation of a dielectric with laser or particle beams of sufficiently high intensity or energy, respectively, ionization processes may transfer electrons from the valence band to the conduction band. The transient characteristics of electron excitation with visible lasers in the intensity regime below $I_L \approx 10^{14}$ W/cm^2 have been studied in Kaiser et al. (2000) and Rethfeld (2004, 2006).

For the case of ion impact on insulating materials, mainly two models of track formation are discussed. The first model expects that along the projectile path the target atoms are fully ionized, leading to repulsive forces between them. The resulting movement of atom is termed "Coulomb explosion" and leads directly to material damage (Fleischer et al., 1967, 1975). In contrast, the "thermal spike model" provides a description of electron heating followed by electron-phonon energy transfer (Toulemonde et al., 2000). This description is based on the two-temperature model (Kaganov et al., 1957; Anisimov et al., 1974). The role of these two processes is not finally clarified; however, both processes may occur successively for certain energy ranges of the impinging ion (Bringa and Johnson, 2002).

In the following we review different mechanisms for phase transitions occurring on different timescales after electronic excitation. The mentioned experiments are performed after laser excitation taking advantage of the large lateral spatial scale of the laser spot. We believe that the microscopic mechanisms in the material are in certain parameter ranges the same as occurring during phase transitions of a solid target after ion bombardment. Thus, studies of laser excitation and the induced processes may provide general insight also to the physical processes induced by heavy ion bombardment.

5.2. Electronically Induced Ultrafast Phase Transitions

As mentioned above, the process of Coulomb explosion is discussed to be responsible for damage of dielectric material irradiated by swift heavy ions (Fleischer et al., 1967; Bringa and Johnson, 2002). This process is initiated by locally high charges occurring after electron excitation leading to ionization of target atoms. Repulsive Coulomb forces may lead to material damage and ablation. For the case of laser irradiation it was found that Coulomb explosion can lead to removal of the top surface layers of excited dielectrics (Stoian et al., 2002; Bulgakova et al., 2004).

For the macroscopic removal of material by this process, a net charge of the surface must be present. If electronic transport rapidly neutralizes the surface region, as may be expected for metals and semiconductors (Bulgakova et al., 2004; Stoian et al., 2004), the material does not disrupt. However, in this case one may speak about a rapid transition to the plasma state at solid density.

Another rapid, directly electronically induced phase transition to the *liquid* state is known for covalently bonded semiconductors. This rapid transition occurs at lower intensities than possible direct transitions to the *plasma* state at solid density, as discussed above. Here, the photo excited high density electron-hole plasma may lead to a lattice instability (Stampfli and Bennemann, 1994), resulting

in a disordering of the lattice and thus a transition to the liquid state on a time scale of approximately 100 fs. This process is often called *non-thermal* melting, since the disordering occurs faster than lattice heating. Experimentally the process of ultrafast non-thermal melting was detected directly by time-resolved X-ray diffraction (Siders et al., 1999; Sokolowski-Tinten et al., 2001).

Also for metals, processes of ultrafast non-thermal melting have been under discussion (Falkovsky and Mishchenko, 1997, 1999), but they are not yet unambiguously demonstrated. Most of the studies claiming the experimental observation of ultrafast melting of metals could be explained with the mechanism of homogeneous melting discussed in the following subsection.

5.3. Thermal Phase Transitions of the Heated Lattice

The typical time scale for thermal lattice heating due to electron-phonon collisions is in the range of a few to tens of picoseconds. However, depending on excitation strength, already a few picoseconds after irradiation the crystal may be strongly superheated, i.e. the lattice temperature greatly exceeds the equilibrium melting temperature (Rethfeld, 2004a). Usually subsequent *thermal* melting is supposed to start at the surface, where the energy barrier for heterogeneous nucleation of a liquid layer at the solid-vapour interface is zero. In this case, a melting front proceeds from the surface into the material with a velocity limited by the speed of sound. A natural limit for the melting time is therefore the thickness of the heated layer divided by the melting front velocity. Typical times for melting by this mechanism of *heterogeneous* nucleation are in the range of about 100 nm/10^3 m/s = 100 ps.

In Rethfeld et al. (2002a) the possibility of laser-induced melting of crystals due to *homogeneous* nucleation was considered. It was shown that a sufficiently superheated bulk crystal would melt completely in less than one picosecond. Thus, the time for homogeneous melting is limited only by the time for lattice heating, and is therefore expected to be longer than the time for non-thermal melting mentioned above, but significantly faster than the time needed for a melting front to sweep from the surface through the heated layer (i.e. heterogeneous melting). Homogeneous melting can thus explain experimental observations of rapid melting of solids without invoking nonthermal mechanisms (Ashitkov et al., 2002; Siwick et al., 2003).

Also molecular dynamic simulations have confirmed the microscopic view of melting by homogeneous nucleation (Jin, 2001). For the case of laser excitation, extended molecular dynamic simulations have shown the dynamics of short-pulse laser-induced melting, studying in detail the interplay of homogeneous and het-

erogeneous melting mechanisms (Ivanov and Zhigilei, 2003a, 2003b; Lorazo et al., 2006).

5.4. Further Phase Transitions

Once the material has lost the crystalline order, further phase transitions are usually connected with a remarkable density decrease. In this case, the timescale of phase transition strongly depends on the spatial dimensions of the heated volume and the position of a possible free surface where expansion may be initiated.

The timescale of expansion can be estimated by dividing the spatial target dimensions with the sound velocity. Typical timescales for the density decrease of laser-heated material are in range of 100 ps. Note that the liquid-gas phase transition is connected with a strong drop of sound velocity, resulting in a complex density profile during expansion (Sokolowski-Tinten et al., 1998; Anisimov et al., 1999; Zhakhovskij et al., 2000).

In the case of ion bombardment of larger volumes, the material in the center of the target can be kept in the state of warm dense matter at solid state density for long times up to the range of 100 ns (Tahir et al., 2005).

6. Summary and Open Problems

The perspectives to use intense ion beams as drivers has initiated many experimental and theoretical programs to investigate ion beam plasma interaction phenomena. It was clearly demonstrated that fully ionized plasma consisting of bare ions is a very effective stopping medium. The stopping power enhancement is almost a factor of 40 for Kr ions at an energy of 45 keV/u passing through a fully ionized hydrogen discharge plasma. This is well explained by the effective energy transfer in collisions with free electrons and the higher charge state of projectile ions in a fully ionized plasma. Enhanced charge states of heavy ions in plasma were observed in experiments and we have a sufficient theoretical modelling for this phenomenon (Nardi and Zinamon, 1982; Boine-Frankenheim and Stockl, 1996). This led to the proposal to use plasma strippers for accelerators, where foil strippers or gas strippers are routinely used to generate ions in high charge states for effective acceleration (Alton et al., 1992; Neuner et al., 1999; Oguri et al., 2000).

It is very difficult to generate a plasma situation of fully ionized ions and free electrons for materials other than hydrogen. In the case of carbon this requires plasma temperatures well above 200 eV, a situation which is expected to prevail in the converter material of a in inertial fusion target. The PHELIX laser system at GSI (Neumayer, 2005) is designed for this experiment. Here the problem is not

the temperature but the fact that the plasma conditions have to be provided in a way to be suitable for ion beam-plasma interaction experiments. To this extend a large focal spot of the order of 1mm with low temperature and density gradients is necessary and this is an experimental challenge, which has not yet been met.

In the situation where the plasma ions still have bound electrons the experimental data base is very small. In the case of z-pinch plasma an enhanced stopping power has been observed, but there are no reliable charge state measurements available. Therefore efforts are underway to revisit the problem of projectile charge states inside matter with new high resolution spectroscopy (Rosmej et al., 2005) and to scale the results to plasma target conditions with less bound electrons, free electrons, changes in binding energies and screening.

For the theoretical description of the charge state distributions, the cross sections must be scaled to plasma target conditions. This allows to simulate the passage through the laser generated plasma, giving information about the charge state history of the projectiles. Combined with the charge dependent stopping powers $S(q)$ for bound electrons together with the energy transfer to the free electron gas a microscopic description of the energy deposition of swift ions in plasmas will be given.

We have reviewed studies on the dynamics of a solid during and after irradiation with an ultrashort laser pulse of moderate intensity. For a pulse duration in the subpicosecond regime, the basic processes as excitation and subsequent phase transitions are temporally separated. We have discussed electronically induced ultrafast "non-thermal" phase transitions as well as mechanisms of thermal phase transitions, following lattice heating. Qualitatively, the results can be directly applied to the studies of ion tracks in solids, where similar mechanisms are discussed. For a quantitative adaptation, the specific geometry and parameter range of ion-solid interaction has to be taken into account.

In future, we will study phase transitions induced by a high-intensity laser and ion beam pulse, transforming the initial solid directly to the plasma state. A detailed understanding of the materials pathway on a nanosecond timescale is essential for the interpretation of time-resolved experiments on the interaction of ions with laser produced plasmas. The initial conditions for corresponding hydrodynamic simulations of laser-matter interaction and plasma expansion must be improved; ideally, also phase transitions should be taken into account. To this end, the transient description of the dynamics of a solid during and after laser irradiation should be provided for a large range of intensities and timescales. Specific features of solid carbon and hydrogen will be studied.

Acknowledgement

We thank C. Trautmann for helpful discussions.

References

Alton G.D., Sparrow R.A. and Olsen, R.E. (1992): Plasma as a high-charge-state projectile stripping medium. Phys Rev A **45, no. 8**, 5957–5963

Anisimov S.I., Kapeliovich B.L. and Perel'man T.L. (1974): Electron emission from metal surfaces exposed to ultrashort laser Pulses. Sov Phys JETP **39**, 375–377

Anisimov S.I., Inogamov N.A., Oparin A.M., Rethfeld B., Yabe T., Ogawa M. and Fortov V.E. (1999): Pulsed laser evaporation: Equation-of-state effects. Appl Phys A **69**, 617–620.

Ashitkov S.I., Agranat M.B., Kondratenko P.S., Anisimov S.I., Fortov V.E., Temnov V.V., Sokolowski-Tinten K., Zhou P. and von der Linde D. (2002): Ultrafast structural transformations in graphite. JETP Lett **75**, 87.

Badger B. et al. (1990): HIBALL – A conceptual heavy ion beam driven fusion reactor study. Kernforschungszentrum Karlsruhe Report KfK-3202

Bethe, H. (1930): Zur Theorie des Durchgangs schneller Korpuskularstrahlen durch Materie. Ann Phys **5**, 324–400

Bethe H.A. (1932): Bremsformel für Elektronen relativistischer Geschwindigkeit. Z Phys **76**, 293

Belyaev G., Basko M., Cherkasov A., Golubev A., Fertman A., Roudskoy I., Savin S., Sharkov B., Turtikov V., Arzumanov A., Borisenko A., Gorlachev I., Lysukhin S., Hoffmann D.H.H. and Tauschwitz A. (1996): Measurement of the Coulomb energy loss by fast protons in a plasma target. Phys Rev E **53, no. 3**, 2701–2707

Blazevic A., Bohlen H.G. and von Oertzen W. (2000): Charge-state changing processes for Ne ions passing through thin carbon foils. Phys Rev A **61**, 032901

Blazevic A., Bohlen H.G. and von Oertzen W. (2002): Stopping power of swift neon ions in dependence on the charge state in the non-equilibrium regime. Nucl Instr Meth Phys Res B **190**, 64.

Bloch F. (1933): The slow down of rapidly moving particles in their passing through solid matter. Ann Phys (Leipzig) **16**, 285–320

Bohlen H.G. (1983): The magnetic spectrometer at VICKSI. In: Symposiom of Detectors in Heavy Ion Reactions, Lecture Notes in Physics, Vol. 178, Springer Verlag, Berlin, pp 105

Bohr N. (1948): The penetration of atomic particles through matter. Mat Phys Medd K Dan Vidensk Selsk **18, no. 8**, 1–144

Boine-Frankenheim O. and Stockl C. (1996): Charge state and nonlinear stopping power of heavy ions in a fully ionized plasma. Laser and Particle Beams **14, no. 4**, 781–788

Bringa E.M. and Johnson R.E. (2002): Coulomb explosion and thermal spikes. Phys Rev Lett **88**, 165501

Bulgakova N.M., Stoian R.,Rosenfeld A., Hertel I.V. and Campbell E.E.B. (2004): Electronic transport and consequences for material removal in ultrafast pulsed laser ablation of materials. Phys Rev B **69**, 054102

Couillard C., Deicas R., Nardin Ph., Beuve M.A., Guihaume J.M., Renaud M., Cukier M., Deutsch C. and Maynard G. (1994): Ionization and stopping of heavy ions in dense laser-ablated plasmas. Phys Rev E **49, no. 2**, 49

Dietrich K.G., Hoffmann D.H.H., Boggasch E., Jacoby J., Wahl H., Elfers M., Haas C.R., Dubenkov V.P. and Golubev A.A. (1992): Charge state of fast heavy-ions in a hydrogen plasma. Phys Rev Lett **69, no. 25**, 3623–3626

Deutsch C., Maynard G., Bimbot R., Gardes D., Dellanegra S., Dumail M., Kubica B., Richard A., Rivet M.F., Servajean A., Fleurier C., Sanba A., Hoffmann D.H.H., Weyrich K. and Wahl H. (1989). Ion beam-plasma interaction – A standard model approach. Nucl Instr Meth Phys Res A **278, no. 1**, 38–43

Falkovsky L.A. and Mishchenko E.G. (1997): Lattice deformation from interaction with electrons heated by ultrashort laser pulse. JETP Lett **66**, 208

Falkovsky L.A. and Mishchenko E.G. (1999): Electron lattice kinetics of metals heated by ultrashort laser pulses. J Exp Theor Phys **88**, 84

Fleischer R.L., Price P.B., Walker R.M. and Hubbard E.L. (1967): Criterion for registration in dielectric track detectors. Phys Rev **156**, 353

Fleischer R.L., Price P.B. and Walker R.M. (1975): Nuclear Tracks in Solids. Principles and Applications, University of California Press, Berkeley, CA

Gardes D., Bimbot R., Dellanegra S., Dumail M., Kubica B., Richard A., Rivet M.F., Servajean A., Fleurier C., Sanba A., Deutsch C., Maynard G., Hoffmann D.H.H., Weyrich K. and Wahl H. (1988): Interaction of heavy-ion beams with a hydrogen plasma – Plasma lens effect and stopping power enhancement. Europhys Lett **7, no. 8**, 701–705

Gardes D., Bimbot R., Dumail M., Kubica B., Richard A., Rivet M.F., Servajean A., Fleurier C., Sanba A., Hong D., Deutsch C., Maynard G., Hoffmann D.H.H., Weyrich K. and Dietrich K.G. (1989): Experimental investigation of beam-plasma interactions enhanced stopping power – Plasma lens effect. Rad Eff Defects Solids **110, nos 1–2**, 49–53

Golubev A., Turtikov V., Fertman A., Roudskoy I., Sharkov B., Geissel M., Neuner U., Roth M., Tauschwitz A., Wahl H., Hoffmann D.H.H., Funk U., Suss W. and Jacoby J. (2001): Experimental investigation of the effective charge state of ions in beam-plasma interaction. Nucl Instr Meth Phys Res A **464, nos 1–3**, 247–252

Hoffmann D.H.H., Weyrich K., Wahl H., Peter T., Meyertervehn J., Jacoby J., Bimbot R., Gardes D., Rivet M.F., Dumail M., Fleurier C., Sanba A., Deutsch C., Maynard G., Noll R., Haas R., Arnold R. and Maurmann S. (1988): Experimental-observation of enhanced stopping of heavy-ions in a hydrogen plasma. Z Phys A **330, no. 3**, 339–340

Hoffmann D.H.H., Weyrich K., Wahl H., Gardés D., Bimbot R and Fleurier C. (1990): Energy loss of heavy ions in a plasma target. Phys Rev A **42**, 2313–2321

Hoffmann D.H.H., Blazevic A., Ni P., Rosmej O., Roth M., Tahir N.A., Tauschwitz A., Udrea S., Varentsov D., Weyrich K. and Maron Y. (2005): Present and future perspectives for high energy density physics with intense heavy ion and laser beams. Laser and Particle Beams **23, no. 1**, 47–53

Hubert F., Bimbot R. and Gauvin H. (1990): Range and stopping power table for 2.5-500 Me V/nuclean heavy ions in solids. At Data Nucl Data Tables **46**, 1–213

ICRU (2005): Stopping of ions heavier than helium, Vol. 73 of ICRU Report. J ICRU **5**, 1–253

Ivanov D.S. and Zhigilei L.V. (2003a): Effect of pressure relaxation on the mechanisms of short-pulse laser melting. Phys Rev Lett **91**, 105701

Ivanov D.S. and Zhigilei L.V. (2003b): Combined atomistic-continuum modeling of short-pulse laser melting and disintegration of metal films. Phys Rev B **68**, 064114

Jacoby J. et al. (1995): Stopping of heavy ions in a hydrogen plasma. Phys Rev Lett **74**, 50

Jin Z.H., Gumbsch P., Lu K. and Ma E. (2001): Melting mechanisms at the limit of superheating. Phys Rev Lett **87**, 055703

Kaganov M.I., Lifshitz I.M. and Tanatarov L.V. (1957): Relaxation between electrons and the crystalline lattice. Sov Phys JETP **4**, 173

Kaiser A., Rethfeld B., Vicanek M. and Simon G. (2000): Microscopical processes in dielectrics absorbing a subpicosecond laser pulse. Phys Rev B **61**, 11437

Kaneko T. (1994): Energy loss of swift projectiles with n ($n \leq 4$) bound electrons. Phys Rev A **49, no. 4**, 2681

Kojima, M., Mitomo, M., Sasaki, T., Hasegawa, J., Ogawa, M. (2002): Charge-state distribution and energy loss of 3.2-MeV oxygen ions in laser plasma produced from solid hydrogen. Laser and Particle Beams **20, no. 3**, 475–478

Lindhard J. and Scharff M. (1961): Energy dissipation by ions in the keV region. Phys Rev **124**, 128–130

Logan B.G., Bangerter R.O., Callahan D.A., Tabak M., Roth M., Perkins L.J. and Caporaso G. (2006). Assessment of potential for ion-driven fast ignition. Fusion Sci Technol **49, no. 3**, 399–411

Lorazo P., Lewis L.J. and Meunier M. (2006): Thermodynamic pathways to melting, ablation, and solidification in absorbing solids under pulsed laser irradiation. Phys Rev B **73**, 134108

Maynard G. et al. (2001): Modeling of swift heavy ions interacting with dense matter. Nucl Instr Meth Phys Res A **64**, 86

Nardi E. and Zinamon Z. (1982): Charge state and slowing of fast ions in a plasma. Phys Rev Lett **49, no. 17**, 1251–1254

Nardi E., Fisher D.V., Roth M., Blazevic A. and Hoffmann D.H.H. (2006): Charge state of Zn projectile ions in partially ionized plasma: Simulations. Laser and Particle Beams **24, no. 1**, 131–141

Neumayer P., Bock R., Borneis S., Brambrink E., Brand H., Caird J., Campbell E.M., Gaul E., Goette S., Haefner C., Hahn T., Heuck H.M., Hoffmann D.H.H., Javorkova D., Kluge H.J., Kuehl T., Kunzer S., Merz T., Onkels E., Perry M.D., Reemts D., Roth M., Samek S., Schaumann G., Schrader F., Seelig W., Tauschwitz A., Thiel R., Ursescu D., Wiewior P., Wittrock U. and Zielbauer B. (2005): Status of PHELIX laser and first experiments. Laser and Particle Beams **23, no. 3**, 385–389

Neuner U., Horioka K., Nakajima M., Ogawa M., Oguri Y., Takizawa M. and Yamauchi S. (1999): Performance of a carbon plasma stripper for intense beams. Fusion Engrg Design **44**, 285–286

Northcliff L.C. and Schilling R.F. (1970): Range and stopping-power tables for heavy ions. Nucl Data Tab A **7**, 233–463

Ogawa H., Katayama I., Sugai I., Haruyama Y., Aoki A ., Tosaki M ., Fukuxawa F., Yoshida K. and Ikegami H. (1992): Charge state dependent energy loss of light ions. Nucl Instr Meth Phys Res B **69**, 108–112

Ogawa H., Sakamoto N., Katayama I., Haruyama Y., Saito M., Yoshida K., Tosaki M., Susuki Y. and Kimura K. (1997): Energy loss of 10 MeV/amu atomic helium in carbon, Nucl Instr Meth Phys Res B **132**, 36–40

Ogawa M., Oguri Y., Neuner U., Nishigori K., Sakumi A., Shibata K., Kobayashi J., Kojima M., Yoshida M. and Hasegawa J. (2001): Laser heated dE/dX experiments in Japan. Nucl Instr Meth Phys Res A **464, nos 1–3**, 72–79

Oguri Y., Tsubuku K., Sakumi A., Shibata K., Sato R., Nishigori K., Hasegawa J. and Ogawa M. (2000): Heavy ion stripping by a highly-ionized laser plasma. Nucl Instr Meth Phys Res A **161**, 155–158

Oguri Y., Hasegawa J., Kaneko J., Ogawa M. and Horioka K. (2005): Stopping of low-energy highly charged ions in dense plasmas. Nucl Instr Meth Phys Res A **544, nos 1–2**: 76–83

Peter T. (1988): Energieverlust von Schwerionenstrahlen in dichten Plasmen. MPQ Report 137

Rethfeld B. (2004): Unified model for the free-electron avalanche in laser-irradiated dielectrics. Phys Rev Lett **92**, 187401

Rethfeld B. (2006): Free-electron generation in laser-irradiated dielectrics. Phys Rev B **73**, 035101

Rethfeld B., Sokolowski-Tinten K., Anisimov S.I. and von der Linde D. (2002a): Ultrafast thermal melting of laser-excited solids by homogeneous nucleation. Phys Rev B **65**, 092103

Rethfeld B., Kaiser A., Vicanek M. and Simon G. (2002b): Ultrafast dynamics of nonequilibrium electrons in metals under femtosecond laser irradiation. Phys Rev B **65**, 214303

Rethfeld B., Sokolowski-Tinten K., Anisimov S.I. and von der Linde D. (2004): Timescales in the response of materials to femtosecond laser excitation. Appl Phys A **79**, 767

Rosmej O.N., Blazevic A., Korostiy S., Bock R., Hoffmann D.H.H., Pikuz S.A., Efremov V.P., Fortov V.E., Fertman A., Mutin T., Pikuz T.A. and Faenov A.Y. (2005): Charge state and stopping dynamics of fast heavy ions in dense matter. Phys Rev A **72, no. 5**, 052901

Roy P.K., Yu S.S., Henestroza E., Anders A., Bieniosek F.M., Coleman J., Eylon S., Greenway W.G., Leitner M., Logan B.G., Waldron W.L., Welch D.R., Thoma C., Sefkow A.B., Gilson E.P., Efthimion P.C. and Davidson R.C. (2005): Drift compression of an intense neutralized ion beam. Phys Rev Lett **95, no. 23**, 234801

Rozet J.P., Stephan C. and Vernhet D. (1996): ETACHA: A programm for calculating charge states at GANIL energies. Nucl Instr Meth Phys Res B **107**, 67

Schiwietz G. and Grande P.L. (1999): A unitary convolution approximation for the impact-parameter dependent electronic energy loss. Nucl Instr Meth Phys Res B **153**, 1–9

Siders C., Cavalleri A., Sokolowski-Tinten K., Toth C., Guo T., Kammler M., Horn von Hoegen M., Wilson K., von der Linde D. and Barty C. (1999): Detection of nonthermal melting by ultrafast x-ray diffraction. Science **286**, 1340

Sigmund P. (1992): Statistical theory of charged-particle stopping and straggling in the presence of charge exchange. Nucl Instr Meth Phys Res B **69**, 113–122

Sigmund P. and Schinner A. (2000): Binary stopping theory for swift heavy ions. J Eur Phys D **12**, 425

Sigmund P. and Schinner A. (2001): Nonperturbative theory of charge-dependent heavy-ion stopping. Physica Scripta T **92**, 222–224

Siwick B.J., Dwyer J.R., Jordan R.E. and Miller R.J.D. (2003): An atomic-level view of melting using femtosecond electron diffraction. Science **302**, 1382

Sharkov B.Y., Alexeev N.N., Basko M.M., Churazov M.D., Koshkarev D.G., Medin S.A., Orlov Y.N. and Suslin V.M. (2005): Power plant design and accelerator technology for heavy ion inertial fusion energy. Nucl Fusion **45, no. 10**, S291–S297

Sokolowski-Tinten K., Bialkowski J., Cavalleri A., von der Linde D., Oparin A., Meyer ter Vehn J. and Anisimov S.I. (1998): Transient states of matter during short pulse laser ablation. Phys Rev Lett **81**, 224

Sokolowski-Tinten K., Blome C., Dietrich C., Tarasevitch A., Horn von Hoegen M., von der Linde D., Cavalleri A., Squier J. and Kammler M. (2001): Femtosecond x-ray measurement of ultrafast melting and large acoustic transients. Phys Rev Lett **87**, 225701

Someya T., Miyazawa K., Kikuchi T. and Kawata S. (200): Direct-indirect mixture implosion in heavy ion fusion. Laser and Particle Beams **24, no. 3**, 359–369

Stampfli P. and Bennemann K.H. (1994): Time dependence of the laser-induced femtosecond lattice instability of Si and GaAs: Role of longitudinal optical distortions. Phys Rev B **49**, 7299

Stoian R., Boyle M., Thoss A., Rosenfeld A., Korn G., Hertel I.V. and Campbell E.E.B. (2002): Laser ablation of dilectrics with temporally shaped femtosecond pulses. Appl Phys Lett **80**, 353

Stoian R., Rosenfeld A., Hertel I.V., Bulgakova N.M. and Campbell E.E.B. (2004): Comment on "Coulomb explosion in femtosecond laser ablation of si(111)" [Appl Phys Lett 82, 4190 (2003)]. Appl Phys Lett **85**, 694

Tahir N.A., Deutsch C., Fortov V.E., Gryaznov V., Hoffmann D.H.H., Kulish M., Lomonosov I.V., Mintsev V., Ni P., Nikolaev D., Piriz A.R., Shilkin N., Spiller P., Shutov A., Temporal M., Ternovoi V., Udrea S. and Varentsov D. (2005): Proposal for the study of thermophysical properties of high-energy-density matter using current and future heavy-ion accelerator facilities at GSI Darmstadt. Phys Rev Lett **95, no. 3**, 035001

Toulemonde M., Dufour Ch., Meftah A. and Paumier E. (2000): Transient thermal processes in heavy ion irradiation of crystalline inorganic insulators. Nucl Instr Meth Phys Res B **166–167**, 903

Weyrich K., Hoffmann D.H.H., Jacoby J., Wahl H., Noll R., Haas R., Kunze H., Bimbot R., Gardes D., Rivet M.F. and Deutsch C. (1989): Energy-loss of heavy-ions in a hydrogen discharge plasma. Nucl Instr Meth Phys Res A **278, no. 1**, 52–55

Winterbon K.B. (1977): Electronic energy loss and charge-state fluctuations of swift ions. Nucl Instr Meth **144**, 311–315

Zhakhovskij V.V., Nishihara K., Anisimov S.I. and Inogamov N.A. (2000): Molecular-dynamics simulation of rarefaction waves in media that can undergo phase transitions. JETP Lett **71**, 167

Ziegler J.F., Biersack J.P. and Littmark U. (1985): The Stopping and Ranges of Ions in Solids. Pergamon Press, New York.